




Numerical Study of Wind Loads on Y Plan-Shaped Tall Building Using CFD

Pradeep K Goyal¹, Sonia Kumari¹, Shivani Singh¹, Rahul Kumar Saroj¹,
Rahul Kumar Meena¹, Ritu Raj^{1*} 

¹ Department of Civil Engineering, Delhi Technological University, Delhi, India.

Received 24 October 2021; Revised 28 December 2021; Accepted 07 January 2022; Published 01 February 2022

Abstract

The increase in the population is at an exponential rate, and the available land is in the form of irregular shapes. That is why irregular shapes are very commonly built. Wind load increases with respect to height, so wind load evolution is necessary for such high-rise structures. Wind forces majorly depend on the plan's cross-sectional shape. Therefore, for an irregular shape, an investigation is needed for tall buildings. This paper demonstrates a detailed study on velocity stream line, external pressure coefficients, pressure distribution on the surfaces of the building and the turbulence kinetic energy for the Y-shaped plan for tall buildings under wind excitation for wind incidence angles of 0° to 180°. k-ε turbulence model is utilized to solve the problem using computational fluid dynamics techniques in ANSYS for terrain category II as per IS: 875 (Part3), 2015. Windward faces in all building models show positive pressure distribution, while the leeward faces are under the effect of negative pressure distribution. Wind load can be reduced on building models by modifying the corners, such as chamfering, rounding, and double recessed. The variation of pressure distribution on different faces of a "Y" plan shaped tall building for 0° and 180° is investigated using ANSYS CFX, and the pressure contours are plotted for all the faces of different "Y" shaped buildings to compute the effect of corner modification on pressure distribution. In this research, it was found that building models with rounded corners are highly efficient in resisting the wind load.

Keywords: CFD; Corner Modifications; k-ε Turbulence Model; Tall Building; Pressure Coefficient.

1. Introduction

At present times, due to urbanization, the available land area is not expanding while the population is growing at an exponential rate, particularly in urban areas. So, there has been a shift in the shape and size of the buildings. From horizontal to vertical development in structures. The high-rise structures that were built during the olden days were of regular shape, but due to the constraints of available land, the construction of high-rise structures has shifted from regular shapes to irregular shapes with a better architectural look. This irregular-shaped building needs a detailed analysis of wind effects on such types of tall buildings. The wind effects can be analyzed with the help of wind tunnel tests or CFD tools. Wind tunnel tests are time-consuming and costly, while CFD tools are easily available and optimum. The devastating nature of wind and earthquake loads are two important factors that are responsible for the failure of tall buildings, and hence this failure can be reduced to a great extent by investigating the stability of the structure for wind loads.

From the outside, an irregularly shaped building with a plan cross-sectional area in the shape of a "Y" shape is ideal because such a structure has a "Y" shaped building with three distinct wings. The "Y" shaped building provides an

* Corresponding author: rituraj@dtu.ac.in

 <http://dx.doi.org/10.28991/CEJ-2022-08-02-06>



© 2022 by the authors. Licensee C.E.J, Tehran, Iran. This article is an open access article distributed under the terms and conditions of the Creative Commons Attribution (CC-BY) license (<http://creativecommons.org/licenses/by/4.0/>).

outside view, avoiding any neighboring apartment from being overlooked, and most such types of building structures are best suited for residential, corporate, and hotel purposes. The center core provides torsional resistance to the structure, while the three corridor wings resist wind-excited shear and moment, resulting in a "Y" shaped building that provides both torsional and lateral rigidity. Because of its great stability in critical wind situations, the "Y" plan shape building also disrupts the formation of large wind vortices on the rear side of the structure.

A fair amount of research has already been carried out on wind effects investigations on tall buildings, such as Franke et al. (2007) [1] provided recommendations for CFD applications in wind engineering and provided the basic outlines to form the domain in ANSYS CFX. Bhattacharya and Dalui (2020) [2] analyzed the effect of wind excited action on numerous surfaces of an "E" plan shaped tall building by varying the wind incidence angle from 0° to 180° using both experimental as well as numerical techniques. Chakraborty et al. (2014) [3] examined the distribution of surface pressure on an "+" plan shaped tall building using a wind tunnel experiment, varying the wind incidence angle from 0° to 45° , and it was observed that certain faces have an unusual pressure distribution on several faces. Mukherjee and Bairagi (2017) [4] investigated the pressure distribution and velocity stream line pattern for "N" shaped high-rise buildings using the k- ϵ turbulence model, which also displayed the wind pressure coefficient. Verma et al. (2015) [5] studied the variation of wind pressure on different surfaces of an Octagonal shaped building using ANSYS Fluent for different wind incidence angles of 0° to 30° at an interval of 15° and a comparison of numerical results with experimental data was presented in both isolated as well as interference conditions. Abdusemed and Ahuja (2015) [6] conducted an experimental study on square and triangular plan shaped tall buildings to study the effect of wind action on various cross-section shapes. It was concluded that all the components of wind load on triangular-shaped models were larger in magnitude as compared to the square-shaped models.

Nagar et al. (2020) [7] studied the effect of wind forces using boundary layer wind tunnel tests on square and "H" plan shaped tall buildings under both isolated conditions as well as interference due to similar tall buildings. Using wind tunnel experiments, the mean wind pressure coefficient was determined for various wind directions, and it was discovered that pressure decreases with increasing wind incidence angle, and the suction produced by the interfering building at full blockage was greater than that produced by the other interfering conditions. Mallick et al. (2018) [8] studied numerically the wind pressure coefficient on "C" shaped building models using ANSYS Fluent and concluded that the geometry of the structure, aspect ratios, orientation, and wind incidence angle all had a significant impact on the pressure distribution of the tall building. Paul and Dalui (2016) [9] investigated the behavior of wind on different faces of the "Z" plan shaped tall building for different wind directions varying from 0° to 150° with an increment of 30° . The force coefficients, pressure coefficients, and wind flow pattern are evaluated for the model, and unsteady vortices are observed in the wake region due to a combined effect of positive and negative pressure on the windward and leeward sides. Gomes et al. (2005) [10] presented the results of the wind tunnel experiment for an irregularly shaped building model having a cross-sectional shape in the form of an "L" or "U" shaped. Due to the interference effect, Mukherjee et al. (2014) [11] conducted a thorough analysis of pressure contours on different faces of a "Y"-shaped tall building. It is observed that the peculiar variation in pressure was observed on some faces. For better visualization of flow characteristics, the flow pattern around the model was also presented for better visualization of flow characteristics. Pal et al. [12] studied experimentally the results of an isolated building using a wind tunnel test. Sanyal and Dalui (2020) [13] performed a detailed analysis on the effect of varying the internal angle between the limbs of a "Y" shaped tall building on mean pressure distribution, force coefficients, and moment coefficients for various models for wind incidence angles ranging from 0° to 180° .

Raj and Ahuja (2013) [14] performed an experimental study on tall buildings with similar floor area by varying the cross-sectional shapes, in wind tunnel and measure the wind forces. The study concluded that base shear, base moments and twisting moments acting on tall building due to wind loads are mainly depend upon wind directions. Kumar and Dalui (2017) [15] compared the pressure distribution on the surfaces of a normal cross plan shaped buildings with angular cross plan shaped buildings which were modified by adjusting the internal angles between limbs by 150° at an interval of 30° . Wind induced responses for angular cross buildings differed significantly from normal cross shaped buildings for different directions of wind flow. Bhattacharyya and Dalui (2020) [16] carried out a comprehensive analysis on an E-plan-shaped building that is asymmetrical around both plan axes by varying wind angles from 0° to 330° at a 30° interval. The investigation was carried out using both experimentally and numerically technique ANSYS. Hansora et al. (2015) [17] investigated the impact of the height to width ratio of a tapered tall building on distribution of mean pressure coefficient across various surfaces of different models of the tall building and found that height to width ratio has a substantial impact on the distribution of wind pressure. Bairagi and Dalui (2018) [18] investigated the pressure and aerodynamic behavior of tall buildings with setback for different wind incidence angles varying from 0° to 180° . Gaur and Raj (2020) [19] presented a case study on square shaped model with corner modification and investigated the wind effects using both numerical and experimental methods. The case study revealed that numerical simulations can be reliable for more complex wind simulations and corner modified building model show better performance to reduce drag force. Pal et al. (2021) [20] experimentally investigated experimentally the wind effects on fish plan shaped building model and discussed the pressure distribution pattern using pressure contours.

Meena et al. [21] studied the basic of different bracing pattern on tall building. Bairagi and Dalui (2018) [22] studied the wind effect on setback building model and observed that the model with setback on both sides is more vulnerable than the model with setback on single side. Nagar et al. (2021) [23] studied experimentally the proximity effects between two plus-plan shaped high-rise buildings. Raj et al. (2020) [24] numerically investigate wind action on "H" plan shaped tall buildings. Kumar and Raj (2021) [25] numerically investigated the pressure distribution on an irregular octagonal plan oval shape building model and a detailed analysis of wind effects is provided in the form of pressure contours. Gaur et al. (2021) [26] evaluated the interference effect on corner configured structures with variable geometry and blockage configurations under wind loads using CFD and it is observed that shielding effect suppress the interference effects on the principal building. Pal and Raj (2021) [27] evaluated the wind induced interference effects on square and fish plan shape building model under various interference conditions and the experiment were carried out in boundary layer wind tunnel test at a length scale of 1:300. Zheng et al. (2021) [28] analyzed the impact of geometrical characteristics of building balconies on near façade wind flow and presented the pressure distribution on various surface that were investigated using CFD. It is investigated the mean wind speed is mostly depends on the balcony space. Cheng et al. (2021) [29] investigated the wind pressure and forces effect on the tall building using wind tunnel test and it is observed that façade may have a significant influence on local wind pressure and aerodynamic forces.

This paper focuses on the variation of pressure coefficients at various faces of a "Y" plan shape building and evaluates the wind flow pattern around the building model. The turbulence intensity and velocity profile are discussed in this research study. A comparative analysis of the above-mentioned parameters for different wind incidence angles (0° and 180°) for the rounded corner modification is demonstrated using graphical plots.

The "Y" shaped tall building model is studied using numerical techniques. ANSYS CFX. This research majorly presents the external pressure coefficient on both the model at 00 and 1800. The validation study is performed on a square plan shape model and the result of mean C_p is compared with various international standards and past experimental studies which present more or less the same results. Most of the studies are still silent about irregularly shaped buildings, and hence the evaluation of wind load effects on tall irregular cross-sectional plan-shaped buildings is required and hence this study was performed. The different results are presented in graphical form.

2. Computational Fluid Dynamics

The numerical analysis in this study was performed using ANSYS CFX. Turbulence model namely $k-\epsilon$ model is used to solve the complex fluid problems because it provides more reliable results when compared with experimental techniques.

2.1. Domain

The Domain i.e., the virtual wind tunnel environment, is set up according to Franke et al. (2007) [28] guidelines, which state that the inlet and side wall of the domain are at $5H$ and the outlet is at $15H$ from the building location, while the top is at $6H$ from the ground, where H is the height of the building model. Domain dimensions are depicted in Figure 1. Such a large domain size allows proper generation of vortices and is necessary to prevent the backflow of wind.

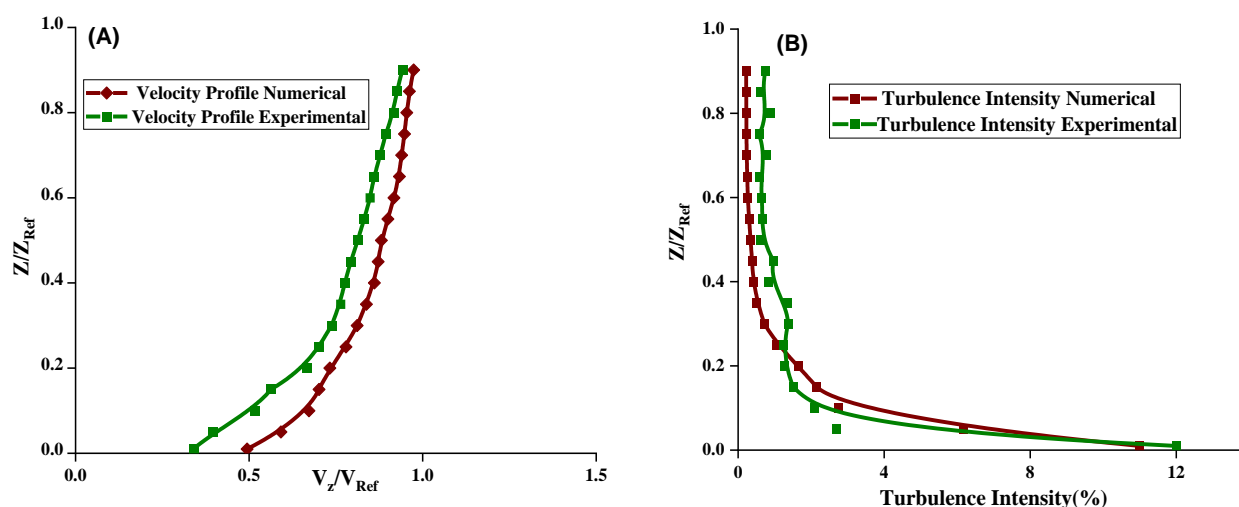


Figure 1. Variation of experimentally [7, 20] and numerically observed (A) Velocity & (B) Turbulence Intensity near the Model

The basic speed at the inlet is provided as per the power law:

$$v_z = v_{Ref} \left(\frac{z}{z_{Ref}} \right)^\alpha \quad (1)$$

where, α is a power law exponent constant which varied as per the terrain category, v_{Ref} is reference velocity which provided as 10 m/s and z_{Ref} is reference height which is 1 m. v_z is velocity at any height z .

The wind velocity profile is governed by the power law equation with the α value of 0.146 which is suitable for terrain category-II of IS 875 (Part-3) 2015 [30]. Since no shear force on the top and side faces of the domain is to be considered, therefore, a free-slip condition is provided here, whereas a no-slip condition is provided on the walls of the building and the bottom face of the domain. The velocity profile and turbulence intensity variation near the building are depicted in Figure 1 where they are also compared with the experimental data observed from wind tunnel experiments.

2.2. Meshing

A tetrahedral type of meshing is provided for the domain as recommended by Chakraborty et al. [30]. Various parameters are explained by Meena et al. [31]. A finer meshing is done on the building and at the domain's base to improve the accuracy of the results obtained for wind parameters. Mesh of 20 layers is provided in the vicinity of the building to provide a smooth flow. To minimize the computation time, uniform coarser tetrahedron meshing is adopted for the whole domain (Figure 2).

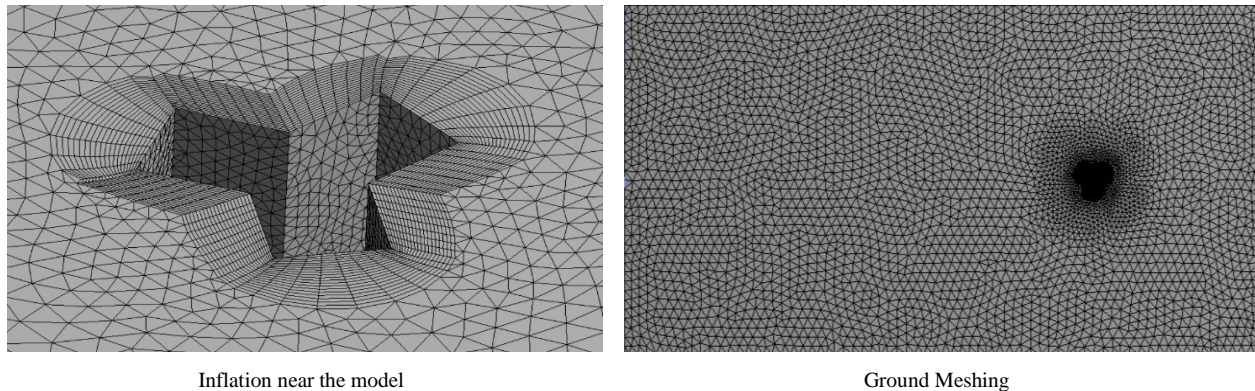


Figure 1. Mesh configuration

3. Research Methodology

3.1. Wind Characteristic

3.1.1. Design Wind Pressure

The wind is a natural current of air moving parallel to the ground, which is caused by uneven heating of the earth's surface by the sun, leading to a difference in the atmospheric pressure. The wind moves from a region of high pressure to a low-pressure region. The wind speed increases with height, from zero at the ground to maximum at the gradient height in the atmospheric boundary layer, and this property is primarily determined by the terrain condition.

When wind strikes a surface, the wind's dynamic energy is converted into pressure. Due to this, it is subjected to forces caused by wind. These forces are called "wind loads." Therefore, it is necessary to study the effect of wind load on buildings to ensure the safety of buildings. Hence, the design wind pressure at any height above mean sea level is evaluated using the below equation to take into account the various safety factors.

$$P_z = 0.6(V_z)^2 \quad (2)$$

$$V_z = V_b \times K_1 \times K_2 \times K_3 \times K_4 \quad (3)$$

where P_z is the pressure of wind in N/m^2 at a height z above mean sea level and V_z refers to the design wind speed in m/s at a height z . V_b is the basic wind speed, K_1 is the Risk Coefficient, K_2 is the Terrain & height factor, K_3 is Topography factor, and K_4 is Importance factor for Cyclic Region.

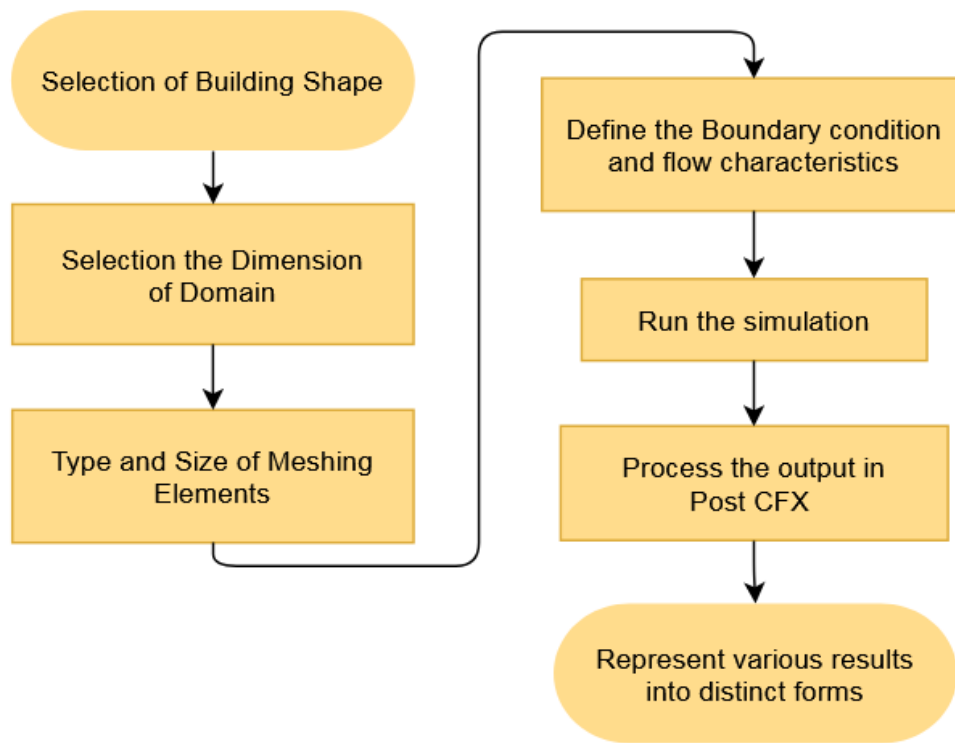


Figure 3. Flow Chart of ANSYS CFX Simulation of Model

3.2. Details of the Turbulence Model

A length scale of 1:100 is used for the modelling of two Y-shaped building models. Model A is a "Y"-shaped building with sharp corners. The dimensions of each arm of the Model A are 200 mm in length and width, with a total height of 600 mm. Figure 4 shows the isometric and top views of Model A.

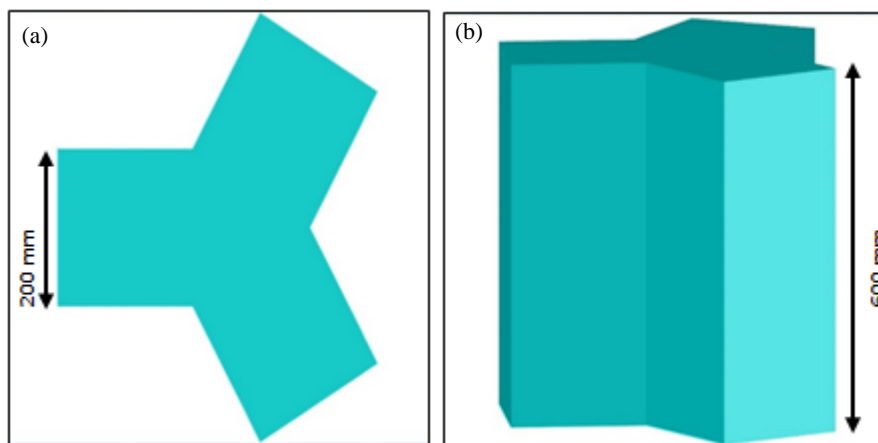


Figure 4. Detailed Dimensions of the model A sharp corners (a) Plan of Y shaped tall building and (b) Isometric view

The corner modified model, Model B is a Rounded corner Y shaped building developing from the fundamental Model A. The cutting radius of corners is taken as 25mm which gives an area reduction of 0.51% as compared to the sharp cornered Model A. Figure 5 demonstrates isometric and top view of Model B.

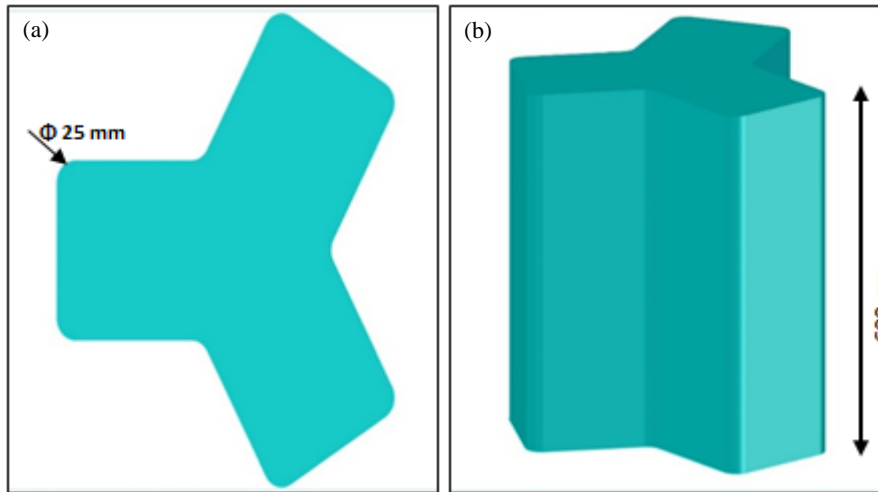


Figure 5. Detailed Dimensions of the model B round corner (a) Y- round corner plan and (b) Isometric view

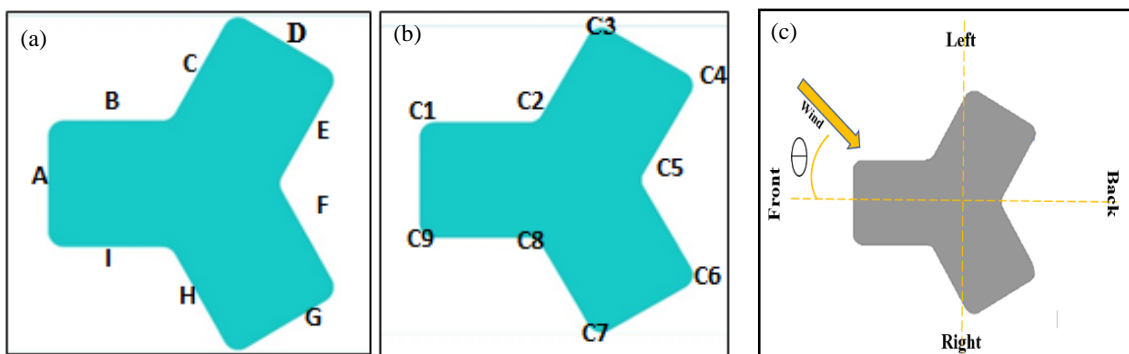


Figure 6. (a) Faces b) Corners (c) Wind orientation

The mean flow characteristics are simulated using a k-ε turbulence model. This model has two equations. For a turbulence model used, instantaneous velocity can be written as the summation of time averaged mean velocity and a time varying fluctuating component given in Equation 4:

$$u_i = U_i + u_i' \tag{4}$$

where, u_i is instantaneous velocity, U_i is time averaged mean velocity, and u_i' is fluctuating component of velocity.

As per Reynold’s Average Navier Stokes Equation (RANS) Equation 2:

$$\frac{\partial}{\partial x_i}(\rho U_i) = 0 \tag{5}$$

where, ρ is the density of fluid and conservation of momentum Equation 3:

$$\frac{\partial}{\partial x_j}(\rho U_i U_j) = -\frac{\partial P}{\partial x_i} + \frac{\partial}{\partial x_f} \left[\mu \left(\frac{\partial U_i}{\partial x_j} + \frac{\partial U_j}{\partial x_i} \right) \right] + \frac{\partial}{\partial x_j} \left(-\rho u_i' u_j' \right) \tag{6}$$

Wind loads on an isolated square-shaped tall building for wind angle 0 are analyzed by the k- ε model, and the corresponding pressure coefficients for different faces are compared with the recommendations given in Indian Standards IS; 875 (pt-3): 2015. A square plan building with height 600mm and width of 200 mm is considered, so the aspect ratio (height/width) is kept 3 and a it is exposed to a wind velocity of 10 m/s. Table 1 depicts the relative comparison between the CFD simulation and the IS Code.

Table 1. Comparative analysis between CFD simulated results and the IS Code

Faces	CFD Simulation	IS- 875 (part 3) 2015
Windward	0.605	0.8
Side Face	-0.56	-0.8
Leeward	-0.198	-0.25

4. Results

ANSYS CFX is utilized to compute the value of C_{pe} i.e. the external pressure coefficient, using the Equation 7:

$$C_{pe} = \frac{P}{0.6 \times V_z^2} \tag{7}$$

where P is Surface Pressure and V_z is Design Wind Speed. The positive value of C_{pe} represents that the wind is directly dissipated at the surface. On the other hand, the negative value C_{pe} represents that due to vortices generation, a suction pressure is created and the flow separation takes place.

4.1. Flow Pattern

The velocity field around the building models for 0 and 180 wind incidence angles for both sharp and rounded corner modification, as obtained from the k-ε method are shown in Figures 7 and 8 respectively. From the flow pattern figure, it is clearly observed that the wind is separating away at the edges of the windward faces and reverts back after that, causing high wind velocity at the corner region of the windward side. For 0° wind incidence angle we can observe, Y-sharp experiences higher wind velocity whereas in case of 180° the wind first strikes the front two faces and before separating away at the edges it reverts back and form eddies thereby creating a local suction and also the wind velocity is higher as compared to 0° case. Y-Round experiences higher wind velocity at windward corners. Since the building is triaxially symmetrical this similar kind of situation will create for wind incidence angle 120° as in case of 0°. Rounded shape experiences maximum velocity at this corner region for all wind incidence angles except for the 0° where sharp corner experiences higher velocity at this corner. For Y- sharp model the size of the eddies are more as compared to Y-round, the round shape of the corner will reduce the size of eddies. As the eddy size is minimum for Y-Rounded it will experience the least wind force.

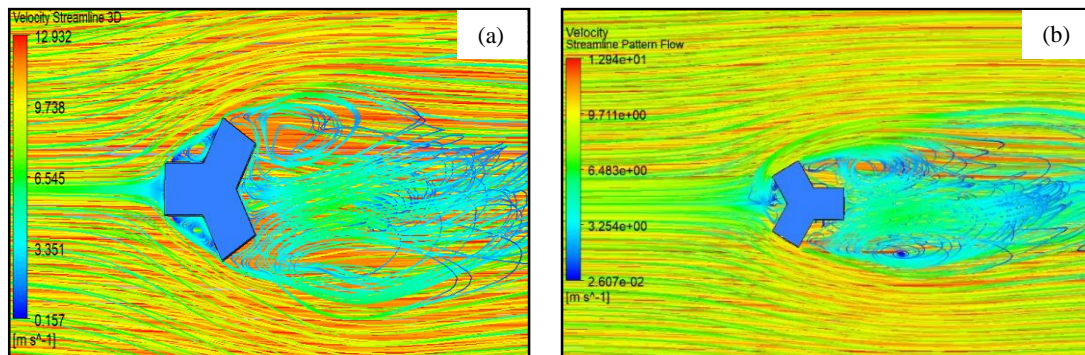


Figure 7. Flow pattern around Model A for (a) 0° and (b) 180° Wind Incidence angle

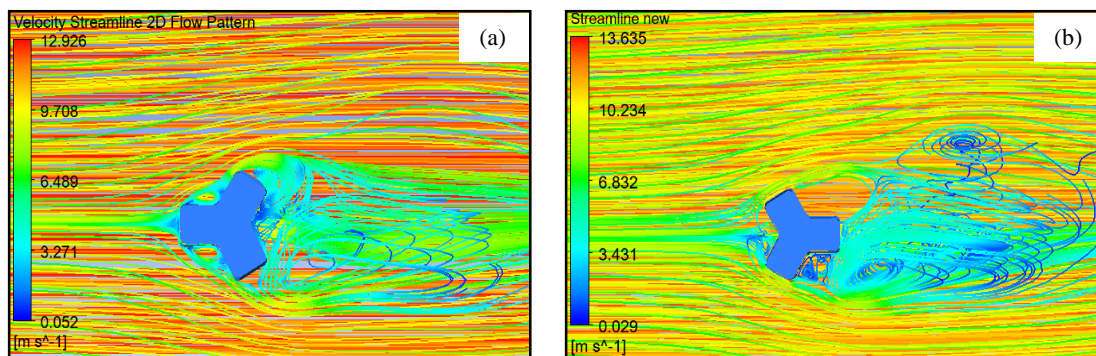


Figure 8. Flow pattern around Model B for (a) 0° and (b) 180° Wind Incidence angle

4.2. Pressure Distribution

The pressure contours for different faces of Model A & B at 0 wind incidence angle is shown by Figures 9 and 10. The pressure contours on the symmetrical faces are identical due to symmetry in wind flow for 0°. On front face, the distribution of pressure is symmetrical about the vertical centerline and it follows a parabolic behavior because of the boundary layer wind flow. There is a positive pressure distribution on faces A, C and H due to direct wind dissipation. At the stagnation point, the highest pressure is observed, which steadily decreases as the flow passes towards the edge of the windward face. After striking against face C, wind reverts back and results in positive pressure on face B. Therefore, Face B is subjected to a lower value of positive pressure because of interference effect of Face C near corner C3. Similarly, face I experiences positive pressure because of interference effect of face H. Because of flow separation and vortex formation, the leeward faces E and F experience a high value of local suction. The major difference in

pressure due to corner modification occurs for corner C4 and C8. A lower value of local suction is observed for Model B due to reduction in the size of vortex for the rounded corners.

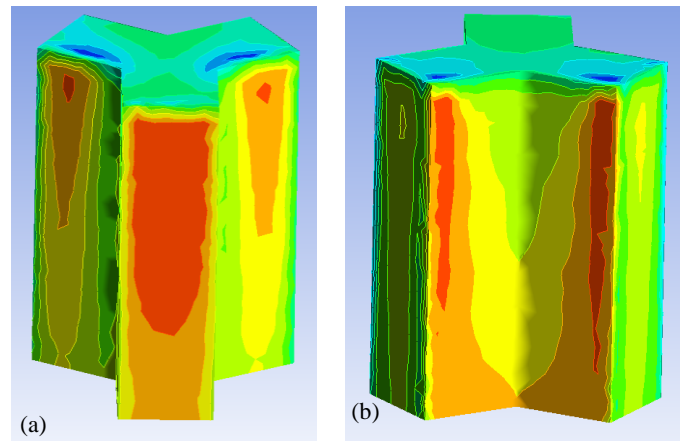


Figure 2. Isometric view of pressure contours for Model A (Y sharp cornered building) for (a) 0° WIA (b) 180° WIA

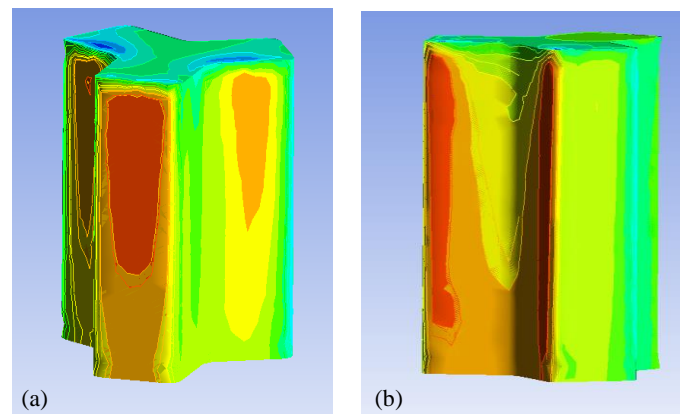
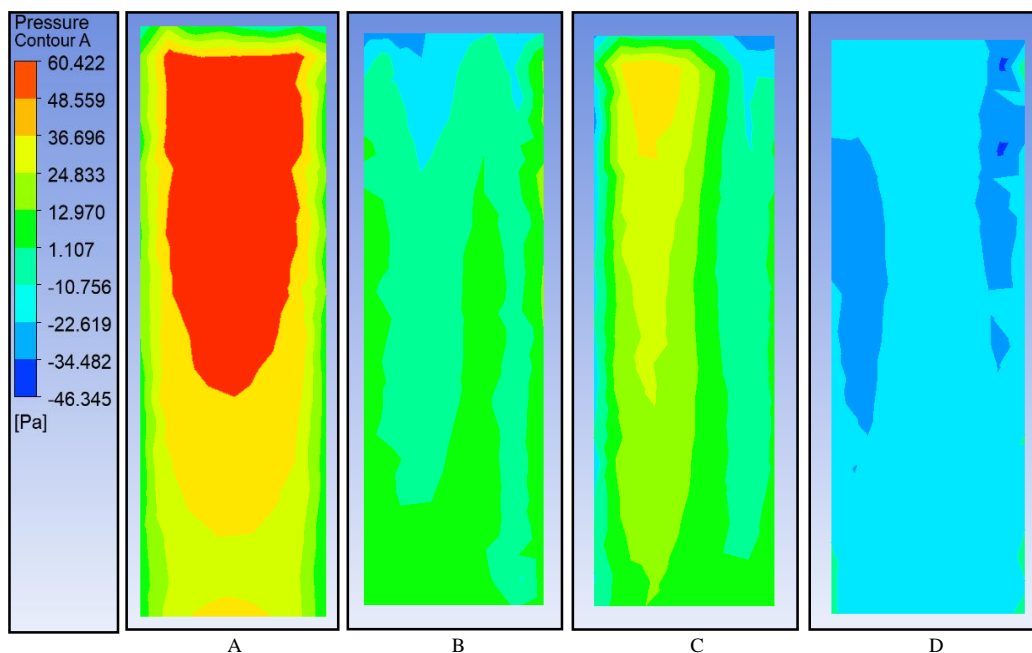


Figure 10. Isometric view of pressure contours for Model B (Y round cornered building) for (a) 0° WIA (b) 180° WIA

The variation of pressure distribution for different wind incidence angles 0° for Model A and Model B are shown by Figures 11 and 12 respectively. Similarly, Figures 13 and 14 represent the pressure distribution for 180° wind incidence angles for Model A and Model B. In case of 180°, Faces D, E, F and G act as windward faces and therefore are exposed to positive pressure distribution whereas Faces A, B and become leeward faces are thus subjected to negative pressure distribution.



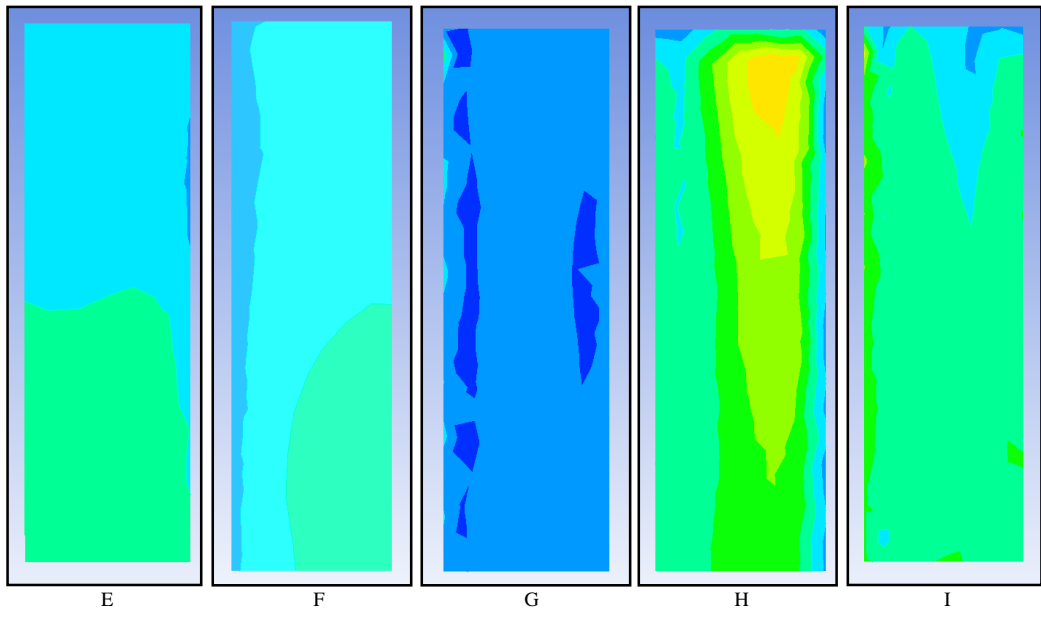


Figure 11. Pressure Contours for different faces of Model A (Y sharp Cornered Building) for 0° WIND

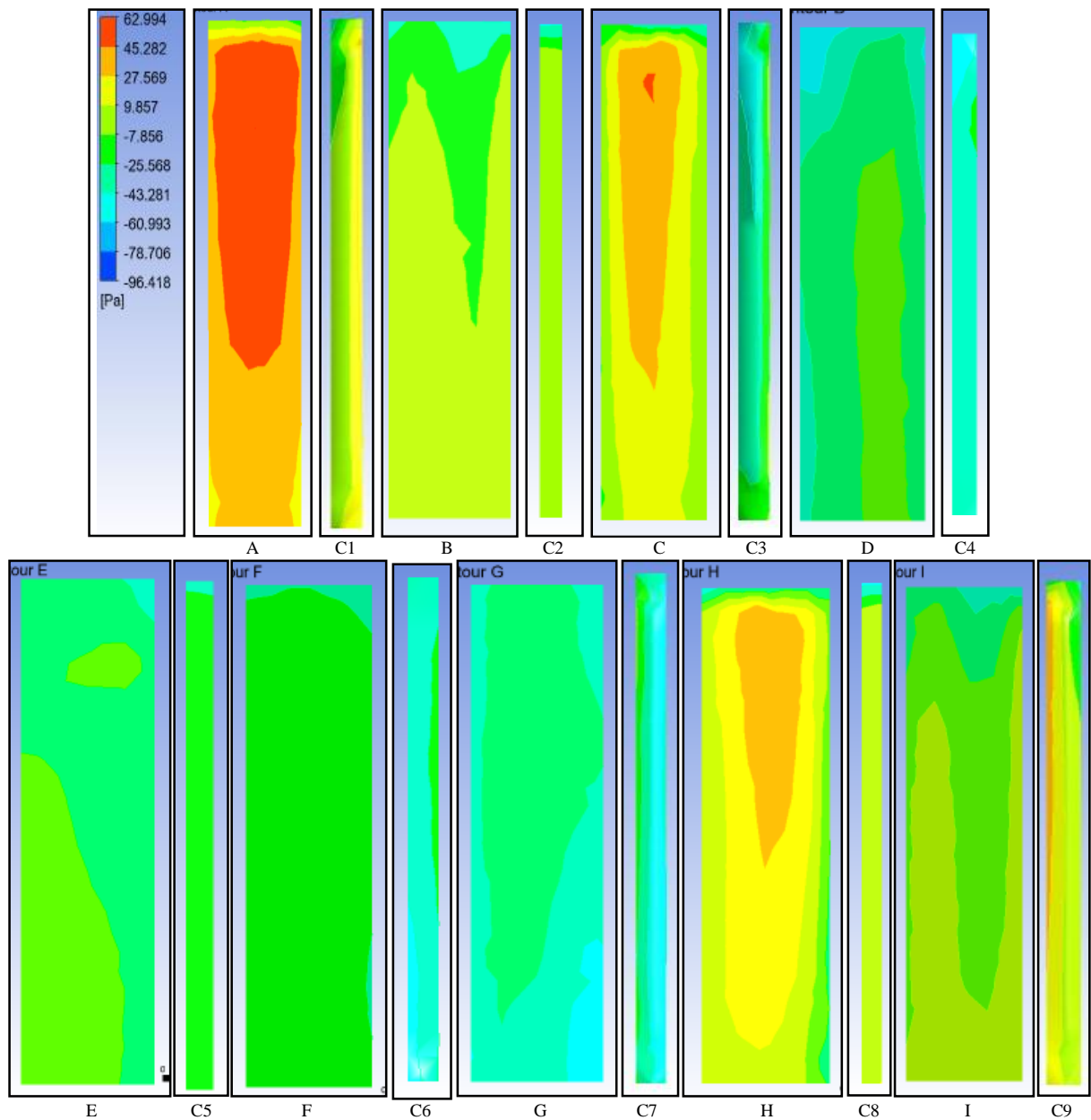


Figure 12. Pressure Contours for different faces and corners of Model B (Y round Cornered Building) for 0° WIND

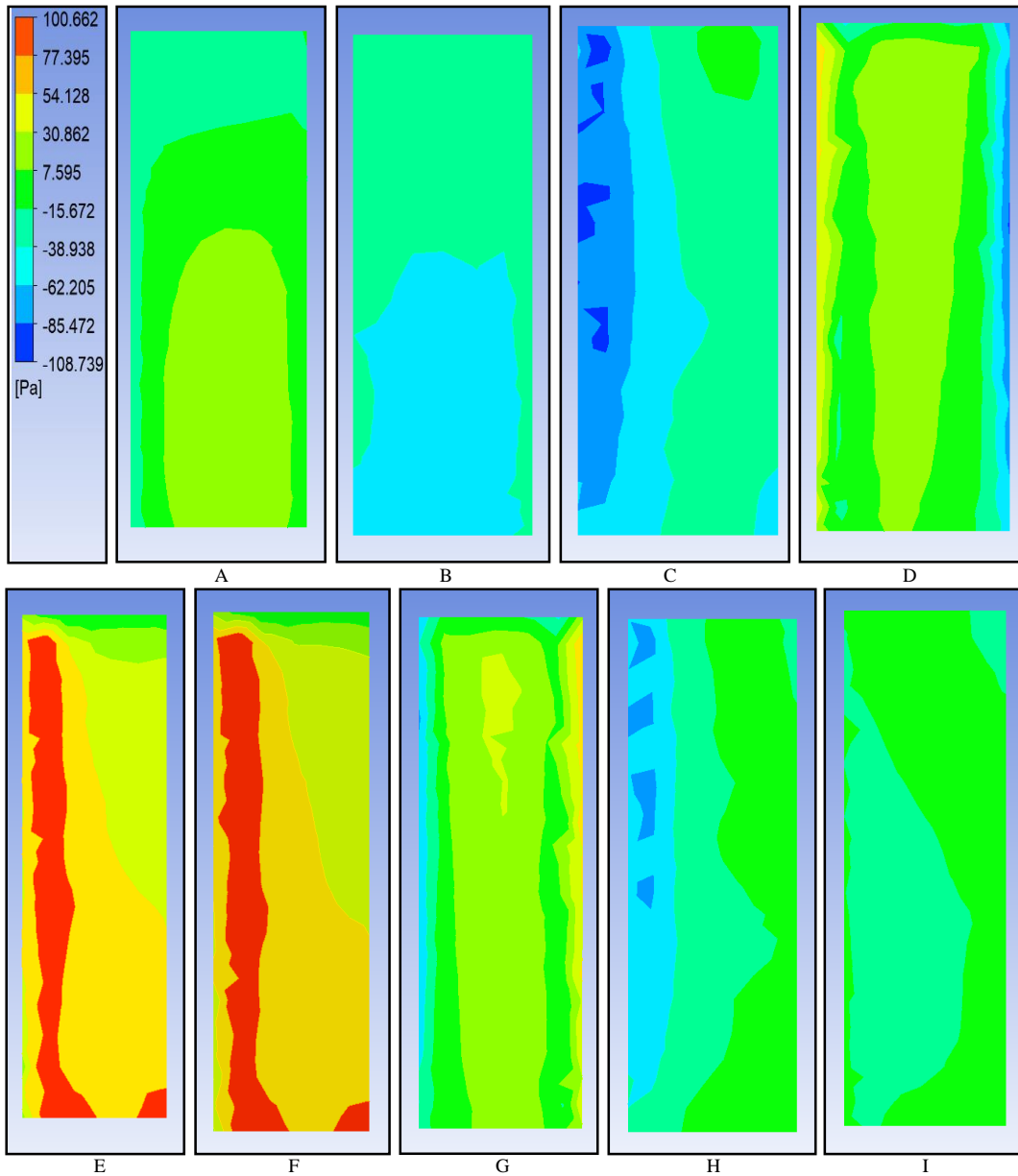
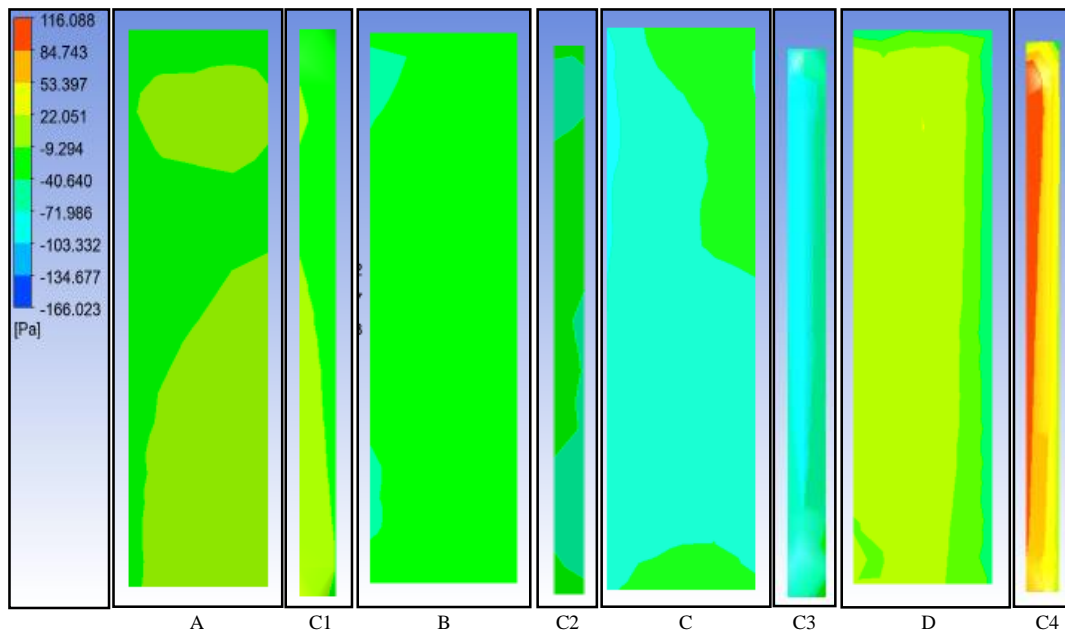


Figure 13. Pressure Contours for different faces of Model A (Y sharp Cornered Building) for 180° WIND



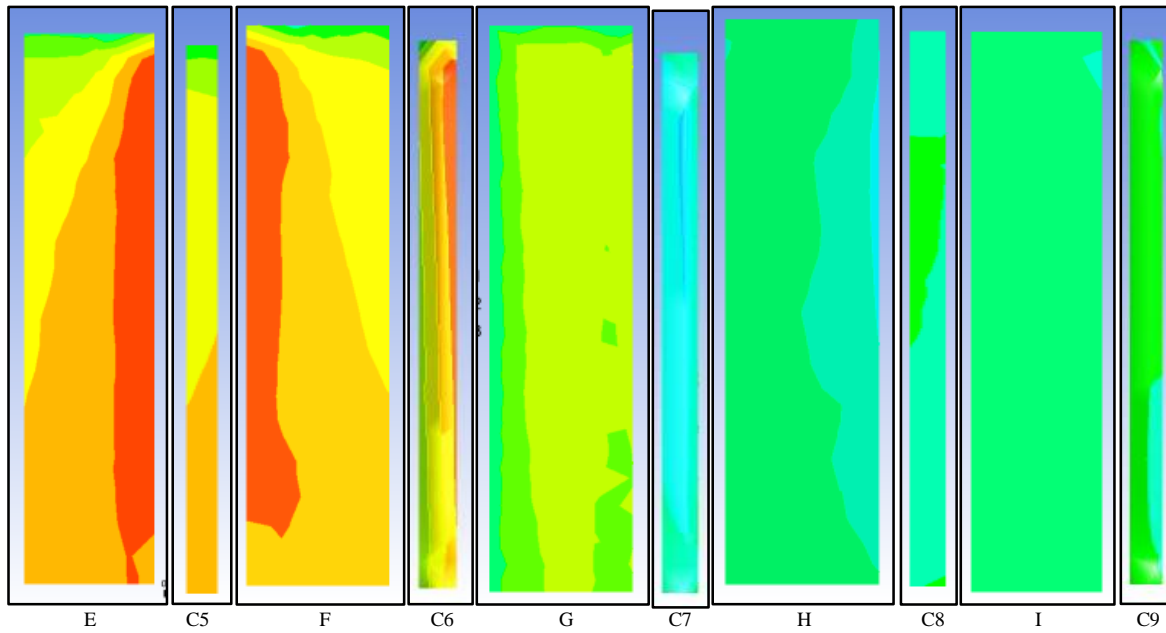


Figure 14. Pressure Contours for different faces and corners of Model B (Y round Cornered Building) for 180° WIND

4.3. Pressure Coefficient

The pressure at any point on the face has been collected for CFD analysis and C_p values of that particular point are calculated. The pressure coefficients of different faces around the building peripheries and at the vertical height of the particular faces are measured and discussed under the following articles.

4.3.1. Vertical C_p for Different Faces and Corners

The graphs shown in Figures 15 to 18 represents the vertical face pressure coefficient at different faces and corners of Model A and B for 0° and 180°. The vertical line has been drawn in the middle of the faces which are parallel to the Z axis and from base to top of the building and the pressure coefficients are measured for different wind angles. The maximum positive mean pressure occurs on Face A for both models for 0° and on face F for 180° wind Incidence angles whereas maximum negative pressure occurs on Face D & symmetrically on face G for 0° for both the models and on face H for 180°. The minimum value of local suction is observed for Model B with rounded corners. This is due to the reduction in the size of vortex at the rounded corner.

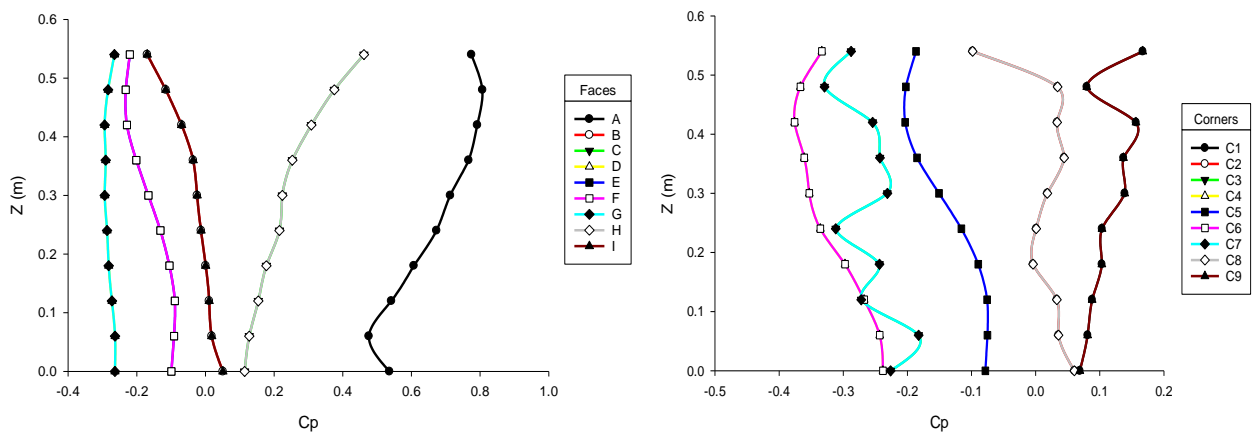


Figure 15. Variation of C_p along vertical centerline for (a) Faces & (b) Corners of Model A for 0° Wind

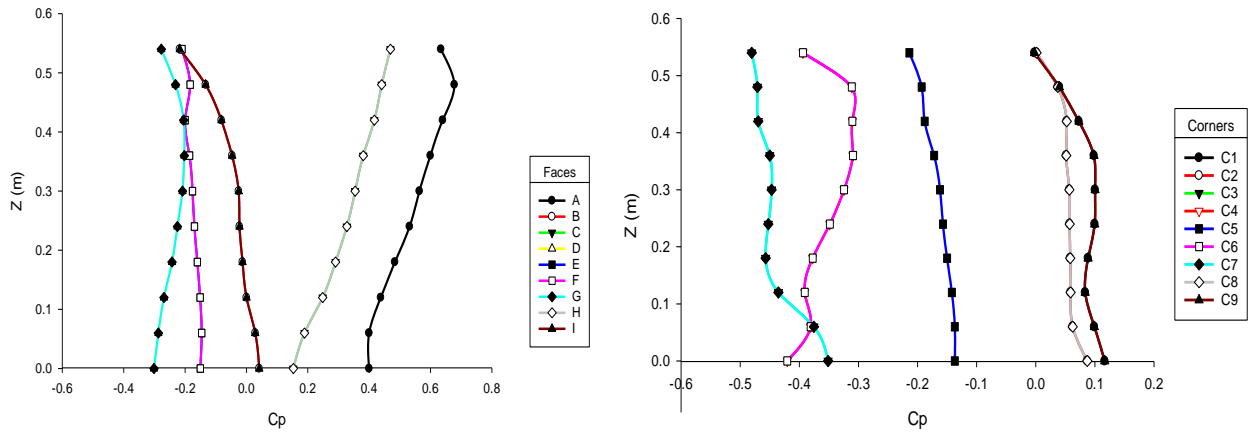


Figure 16. Variation of C_p along vertical centerline for (a) Faces & (b) Corners of Model B for 0° Wind

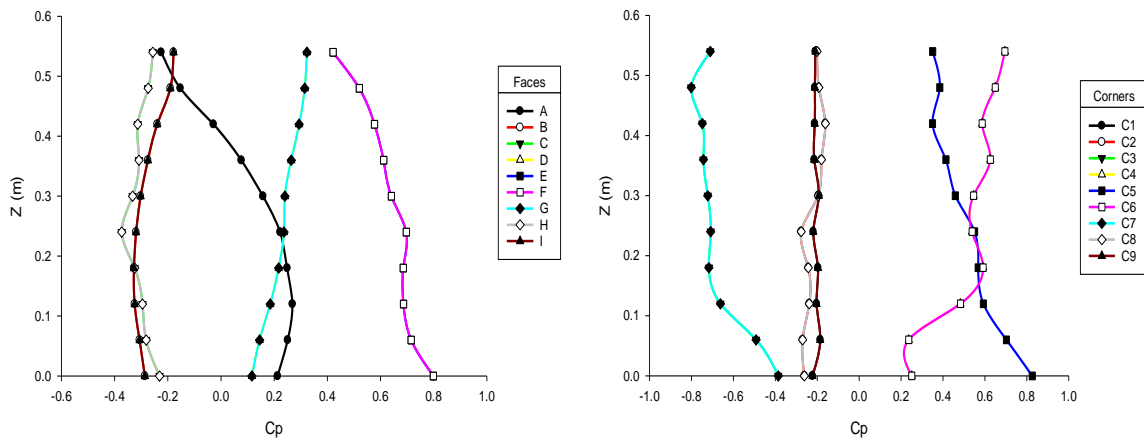


Figure 17. Variation of C_p along vertical centerline for (a) Faces & (b) Corners of Model A for 180° Wind

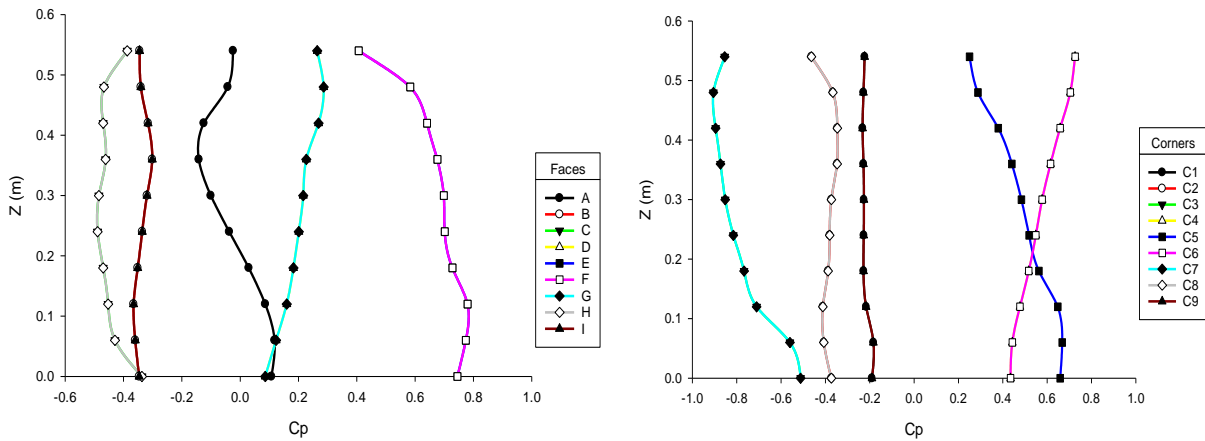


Figure 18. Variation of C_p along vertical centreline for (a) Faces & (b) Corners of Model B for 180° Wind

In both Models Corner 4 & 6 shows the maximum value of local suction and corner 1 & 9 shows maximum positive pressure for 0° whereas in case of 180° corner 7 shows maximum value of local suction and corner 2 shows maximum positive pressure. Model A shows relatively higher values for both suction and positive C_p at faces as well as for corners when compared with the Model B. Therefore, Model B is more efficient in terms of pressure distribution as compared to Model A.

5.3.2. Horizontal C_p around the Building

Horizontal external pressure coefficient (C_p) is also evaluated in this study around the perimeter of the Y-plan shape tall building at a height of $H/2$ from the base of the model for 0° to 180° wind incidence angles. Horizontal line around the perimeter of the building has been drawn from the edge point, namely “C1” and passes through the faces of A B C D E F G H I. From the Figure 19 it can be clearly observed that at 0° wind angle, major increase in negative pressure occurs in the corner portions (C3 and C7) of the building models. And this effect increases when Corner modification is provided. On the other hand, the lesser value of suction on windward side and lesser positive value of C_{pe} on wake

region makes the Model B more stable. For 0° wind incidence angle faces B and I are subjected to positive pressure distribution due to interference effect from face C and H and similar kind of interference effect for these faces has been demonstrated in research study performed by Mukherjee et al. (2014) [11]. Such effect is also observed for 180° incidence angle for face C and I. For the analysis of the Pressure Coefficient, the average C_p of each face of the two models is calculated, and it is deduced that the maximum C_p for rounded model is 30% less than the Y sharp-cornered model however 21% deduction is observed in study presented in Sanyal et al. (2020) [12].

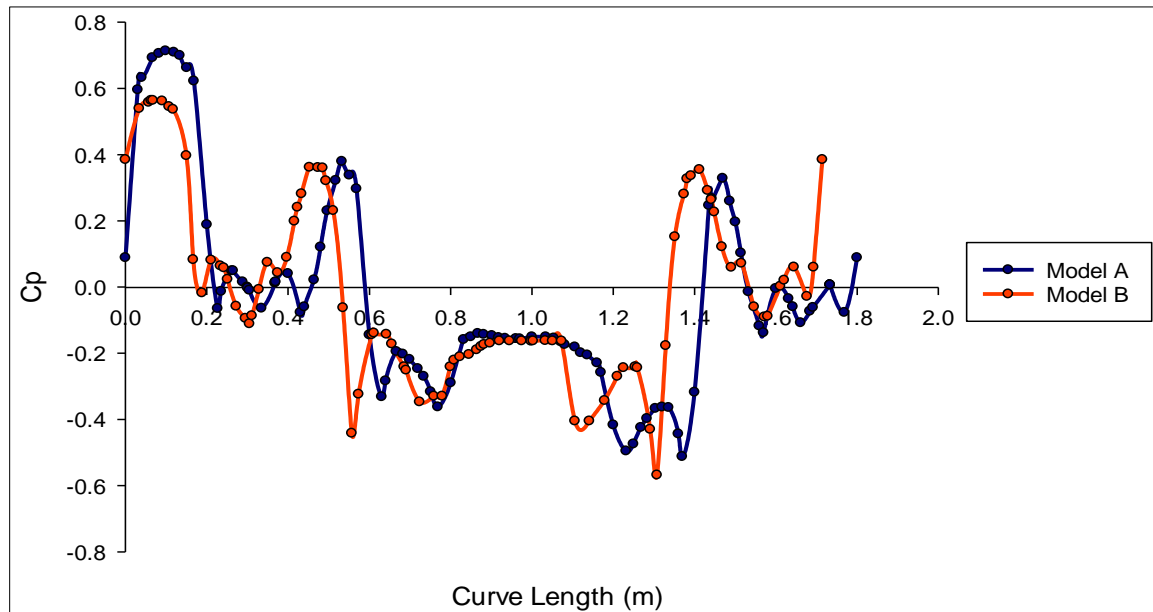


Figure 19. Variation of C_p along Horizontal centerline of Model A and Model B for 0° Wind

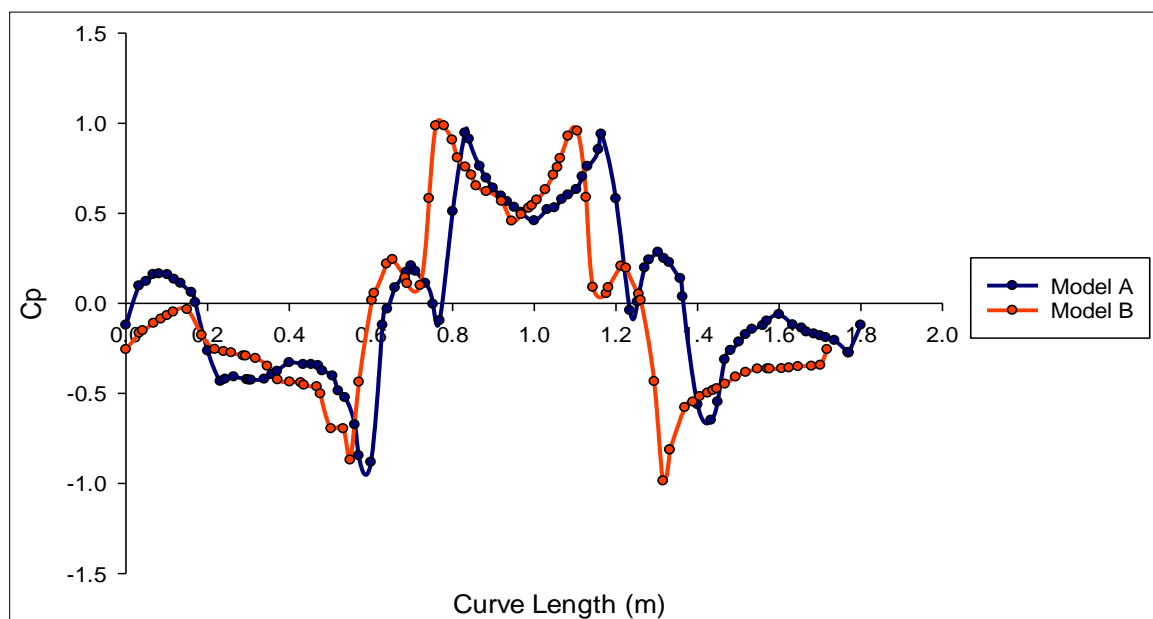


Figure 20. Variation of C_p along Horizontal centerline of Model A and Model B for 180° Wind

5. Conclusions

In this paper, a numerical study has been performed to analyze the wind parameters of a Y-shaped model. An alternative is evaluated to decrease the wind load on the Y-shaped building without compromising the actual height by the introduction of corner modification. Below are the significant conclusions drawn from this study:

- The highest value of wind velocity is obtained at the edges of the windward side and the minimum at the leeward side. Furthermore, after introducing corner modifications, rounded corners on the windward side show the highest speed. Also, the reduced size of the eddy in the case of a rounded model makes model B stable.
- From the study of pressure contours, it is evident that the windward faces are subjected to a positive pressure

distribution due to direct wind dissipation, whereas the leeward faces are subjected to a negative pressure distribution because of flow separation and vortex formation. A lower value of local suction is observed in the case of rounded corners when compared with sharp corners. This is due to the reduction in the size of the vortex at the rounded corners. Therefore, Model B is more efficient in terms of pressure distribution as compared to Model A.

- For a 0° wind incidence angle, faces B and I are subjected to positive pressure distribution due to the interference effect from faces C and H. Such an effect is also observed for the 180° incidence angle for faces C and I.
- For the analysis of the pressure coefficient, the average C_p of each face of the two models is calculated, and it is deduced that the maximum C_p for the rounded model is 30% less than the Y-sharp-cornered model. The rounded corner model showed a lower value of average local suction for any face compared with the normal sharp-cornered model.

Therefore, from this study, the introduction of rounded corner modification on tall buildings is highly efficient in decreasing the wind load and making the structure more stable.

6. Declarations

6.1. Author Contributions

Conceptualization, R.R. and R.K.M.; methodology, R.R., R.K.M., and S.K.; software, S.S. and R.K.S.; validation, R.R., R.K.M. and S.K.; formal analysis, S.S. and R.K.S.; investigation, S.K., S.S. and R.K.S.; resources, R.R. and P.K.G.; data curation, R.R.; writing—original draft preparation, S.K., S.S. and R.K.S.; writing—review and editing, S.K., R.K.M. and R.R.; visualization, R.K.M. and R.R.; supervision, R.R. and P.K.G.; project administration, R.R. and P.K.G.; funding acquisition, R.R. and P.K.G. All authors have read and agreed to the published version of the manuscript.

6.2. Data Availability Statement

The data presented in this study are available in article.

6.3. Funding and Acknowledgements

Authors would like to express their sincere gratitude to Delhi Technological University, Delhi, India for providing funding to conduct the research work.

6.4. Conflicts of Interest

The authors declare no conflict of interest.

7. References

- [1] Franke, J., Hellsten, A., Schlünzen, H., & Carissimo, B. (2007). Guideline for the CFD simulation of flows in the urban environment: COST Action 732 Quality Assurance and Improvement of Microscale Meteorological. Belgium: COST Office.
- [2] Bhattacharyya, B., & Dalui, S. K. (2020). Experimental and Numerical Study of Wind-Pressure Distribution on Irregular-Plan-Shaped Building. *Journal of Structural Engineering*, 146(7), 04020137. doi:10.1061/(asce)st.1943-541x.0002686.
- [3] Chakraborty, S., Dalui, S. K., & Ahuja, A. K. (2014). Experimental investigation of surface pressure on “+” plan shape tall building. *Jordan Journal of Civil Engineering*, 8(3), 251–262.
- [4] Mukherjee, A., & Bairagi, A. K. (2017). Wind pressure and velocity pattern around “N” plan shape tall building-A case study. *Asian Journal of Civil Engineering*, 18(8), 1241–1258.
- [5] Verma, D. S. K., Roy, A. ., Lather, S., & Sood, M. (2015). CFD Simulation for Wind Load on Octagonal Tall Buildings. *International Journal of Engineering Trends and Technology*, 24(4), 211–216. doi:10.14445/22315381/ijett-v24p239.
- [6] Ahuja, A. K., & Gupta, P. K. (2015). Wind Loads on Tall Buildings. *International Journal of Engineering & Applied Sciences*, 1(May), 1–21.
- [7] Nagar, S. K., Raj, R., & Dev, N. (2020). Experimental study of wind-induced pressures on tall buildings of different shapes. *Wind and Structures, An International Journal*, 31(5), 441–453. doi:10.12989/was.2020.31.5.431.
- [8] Mallick, M., Mohanta, A., Kumar, A., & Raj, V. (2018). Modelling of Wind Pressure Coefficients on C-Shaped Building Models. *Modelling and Simulation in Engineering*, 2018. doi:10.1155/2018/6524945.
- [9] Paul, R., & Dalui, S. K. (2016). Wind effects on ‘Z’ plan-shaped tall building: a case study. *International Journal of Advanced Structural Engineering*, 8(3), 319–335. doi:10.1007/s40091-016-0134-9.

- [10] Gomes, M. G., Moret Rodrigues, A., & Mendes, P. (2005). Experimental and numerical study of wind pressures on irregular-plan shapes. *Journal of Wind Engineering and Industrial Aerodynamics*, 93(10), 741–756. doi:10.1016/j.jweia.2005.08.008.
- [11] Mukherjee, S., Chakraborty, S., Dalui, S. K., & Ahuja, A. K. (2014). Wind induced pressure on “Y” plan shape tall building. *Wind and Structures, An International Journal*, 19(5), 523–540. doi:10.12989/was.2014.19.5.523.
- [12] Pal, S., Meena, R. K., Raj, R., & Anbukumar, S. (2021). Wind tunnel study of a fish - plan shape model under different isolated wind incidences, *Wind and Structures*, 33(5). 353-366. doi: 10.12989/was.2021.33.5.353.
- [13] Sanyal, P., & Dalui, S. K. (2021). Effects of internal angle between limbs of “Y” plan shaped tall building under wind load. *Journal of Building Engineering*, 33, 101843. doi:10.1016/j.jobe.2020.101843.
- [14] Raj, R., & Ahuja, A. K. (2013). Wind loads on cross shape tall buildings. *Journal of Academia and Industrial Research*, 2(2), 111-113.
- [15] Kumar, D., & Dalui, S. K. (2017). Effect of internal angles between limbs of cross plan shaped tall building under wind load. *Wind and Structures, An International Journal*, 24(2), 95–118. doi:10.12989/was.2017.24.2.095.
- [16] Bhattacharyya, B., & Dalui, S. K. (2018). Investigation of mean wind pressures on ‘E’ plan shaped tall building. *Wind and Structures, An International Journal*, 26(2), 99–114. doi:10.12989/was.2018.26.2.099.
- [17] Hansora, A. G., Nimodiya, P. N., & Gehlot, K. (2015). Numerical Analysis of Wind loads on Tapered Shape Tall Buildings. *International Journal of Science Technology & Engineering*, 1(11), 92–97.
- [18] Bairagi, A. K., & Dalui, S. K. (2018). Aerodynamic effects on setback tall building using CFD simulation. *International Journal of Mechanical and Production Engineering Research and Development*, June, 413–420.
- [19] Gaur, N., & Raj, R. (2021). Aerodynamic mitigation by corner modification on square model under wind loads employing CFD and wind tunnel. *Ain Shams Engineering Journal*, 13(1), 283. doi:10.1016/j.asej.2021.06.007.
- [20] Pal, S., Raj, R., & Anbukumar, S. (2021). Bilateral interference of wind loads induced on duplicate building models of various shapes. *Latin American Journal of Solids and Structures*, 18(5). doi:10.1590/1679-78256595.
- [21] Meena, R. K., Awadhiya, G. P., Paswan, A. P., & Jayant, H. K. (2021). Effects of Bracing System on Multistoreyed Steel Building. *IOP Conference Series: Materials Science and Engineering*, 1128(1), 012017. doi:10.1088/1757-899x/1128/1/012017.
- [22] Bairagi, A. K., & Dalui, S. K. (2018). Comparison of Pressure Coefficient between Square and Setback. In *SEC18: Proceedings of the 11th Structural Engineering Convention - 2018 Jadavpur University, Kolkata, India*.
- [23] Nagar, S. K., Raj, R., & Dev, N. (2021). Proximity effects between two plus-plan shaped high-rise buildings on mean and RMS pressure coefficients. *Scientia Iranica*, 0(0), 0–0. doi:10.24200/sci.2021.55928.4484.
- [24] Raj, R., Rana, T., Anchalia, T., & Khola, U. (2020). Numerical study of wind excited action on H Plan-shaped tall building. *International Journal on Emerging Technologies*, 11(3), 591–605.
- [25] Kumar, A., & Raj, R. (2021). Study of pressure distribution on an irregular octagonal plan oval-shape building using cfd. *Civil Engineering Journal (Iran)*, 7(10), 1787–1805. doi:10.28991/cej-2021-03091760.
- [26] Gaur, N., Raj, R., & Goyal, P. K. (2021). Interference effect on corner-configured structures with variable geometry and blockage configurations under wind loads using CFD. *Asian Journal of Civil Engineering*, 22(8), 1607–1623. doi:10.1007/s42107-021-00400-0.
- [27] Pal, S., & Raj, R. (2021). Evaluation of Wind Induced Interference Effects on Shape Remodeled Tall Buildings. *Arabian Journal for Science and Engineering*, 46(11), 11425–11445. doi:10.1007/s13369-021-05923-x.
- [28] Zheng, X., Montazeri, H., & Blocken, B. (2021). CFD analysis of the impact of geometrical characteristics of building balconies on near-façade wind flow and surface pressure. *Building and Environment*, 200, 107904. doi:10.1016/j.buildenv.2021.107904.
- [29] Cheng, X., Huang, G., Yang, Q., & Zhou, X. (2021). Influence of Architectural Facades on Wind Pressures and Aerodynamic Forces of Tall Buildings. *Journal of Structural Engineering*, 147(1), 04020303. doi:10.1061/(asce)st.1943-541x.0002867.
- [30] IS:875. (2015). Indian Standard design loads (other than earthquake) for Buildings and Structures. Part 3: Wind Loads (Third Revision). In BIS, New Delhi, India.
- [31] Meena, R. K., Raj, R., & Anbukumar, S. (2021). Numerical Investigation of Wind Load on Side Ratio of High-Rise Buildings. *Advances in Construction Materials and Sustainable Environment*, 937–951. doi:10.1007/978-981-16-6557-8_76.